

Contrastive-SDXL: Annotation-Preserving Night-Time Augmentation for Pedestrian Detection

Franky George, Muhammad Khalid, Adil Khan

Abstract—Night-time pedestrian detection remains challenging because labelled night-time data are limited and large illumination differences make daytime-only trained detectors unreliable. Latent diffusion models (LDMs) provide a powerful basis for image-to-image translation and cross-domain augmentation, but their effectiveness in safety-critical perception depends on whether detector-relevant objects and local semantic structure are preserved when translating between source and target domains. In this work, we present Contrastive-SDXL, a day-to-night augmentation framework for night-time pedestrian detection built on SDXL-Turbo and fine-tuned using Low-Rank Adaptation (LoRA). To preserve semantic correspondence between daytime inputs and translated night-time images, we introduce a patch-wise semantic contrastive loss guided by a pretrained DINOv2 encoder rather than generator encoder features. Multi-level DINOv2 self-attention maps enforce both local and global semantic consistency, while an object consistency loss explicitly encourages pedestrian preservation. Contrastive-SDXL produces realistic night-time images, achieving a Fréchet Inception Distance (FID) of 22.5. Detectors trained with our synthetic images obtain a 6–7% reduction in miss rate compared with a daytime-only baseline, approaching the performance of detectors trained on real night-time data. These results demonstrate that consistency-driven diffusion augmentation can effectively support safety-critical night-time pedestrian detection.

Index Terms—Artificial intelligence, autonomous driving, computer vision, data augmentation, image processing, pedestrian detection.

I. INTRODUCTION

Night-time pedestrian detection remains a critical challenge for autonomous vehicles and advanced driver-assistance systems (ADAS). Although pedestrian detectors have improved substantially under daytime and favourable lighting conditions, their performance often degrades in low-light environments due to reduced visibility, glare, noise, and large illumination differences. This is particularly problematic in safety-critical transportation scenarios, where missed pedestrians can have severe consequences. One direct solution is to collect and annotate large-scale night-time datasets, but this process is costly, time-consuming, and difficult to scale across different locations, weather conditions, and traffic scenes.

Cross-domain augmentation offers an attractive alternative. Instead of collecting and annotating new night-time data, labelled daytime images can be translated into night-style images while reusing their original annotations. A promising direction is diffusion-based image-to-image translation. Diffusion models have recently emerged as powerful generative models, capable of producing high-quality, high-resolution images

across diverse domains. With improvements in generation quality and computational efficiency, state-of-the-art latent diffusion models (LDMs) can now generate photorealistic images that are often difficult to distinguish from real samples. This raises an important question for safety-critical perception tasks: can diffusion-based image-to-image translation be used to convert images from a data-abundant source domain to a data-scarce target domain while preserving the object-level consistency required for detection?

Works such as Palette and SDEdit [1], [2] showed that diffusion models can generate target-style images while preserving source content. However, most existing studies focus on generic visual transformations and perceptual quality, rather than examining whether diffusion-generated images are suitable for safety-critical object detection. This limitation is especially important for day-to-night pedestrian augmentation. Unlike generic image synthesis or style transfer, in a pedestrian detection setting, the translated image must preserve small, occluded, and cluttered pedestrians with sufficient fidelity for the original bounding-box annotations to remain valid. If a pedestrian is distorted, removed, or shifted during translation, the inherited annotation may become unreliable and the downstream detector may learn incorrect cues.

This work addresses this gap in two ways. First, we assess pretrained LDMs as cross-domain augmentation tools for night-time pedestrian detection, focusing on whether synthetic night-time pedestrian images generated from daytime inputs can improve robustness under low-light conditions. Since existing datasets are often biased toward clear lighting and favourable weather, generating night-time images that preserve pedestrian details and scene context could enhance detector training while reducing dependence on newly collected night-time data.

Second, and as our main contribution, we propose Contrastive-SDXL, a framework tailored for safety-critical day-to-night augmentation. Built on SDXL-Turbo [3], our method is fine-tuned using Low-Rank Adaptation (LoRA) [4] and guided by a patch-wise semantic contrastive loss [5] to preserve local and global semantic consistency. Unlike prior unpaired image-to-image approaches that rely on generator encoder features, Contrastive-SDXL uses a pretrained DINOv2 [6] encoder to guide contrastive learning across multiple spatial scales. We further introduce an object consistency loss to explicitly enforce pedestrian preservation during translation.

Experimental results show that Contrastive-SDXL generates visually coherent night-time images while retaining pedestrian structure and scene context. Detectors trained with our synthetic images perform comparably to those trained on real night-time data, demonstrating the effectiveness of consistency-driven

diffusion augmentation for night-time pedestrian perception. Our main contributions are:

- We investigate pretrained LDMs as cross-domain augmentation tools for safety-critical night-time pedestrian detection.
- We propose Contrastive-SDXL, an SDXL-Turbo-based day-to-night translation framework fine-tuned with LoRA and guided by DINOv2-based patch-wise semantic contrastive learning.
- We introduce an object consistency loss to explicitly preserve pedestrians and maintain annotation validity during day-to-night translation.
- We show that Contrastive-SDXL improves low-light detector robustness, achieving a 6–7% reduction in miss rate over a daytime-only baseline and approaching real night training performance.

II. RELATED WORKS

A. Night-time pedestrian augmentation

Pedestrian detection is a core perception task for autonomous vehicles and ADAS, but its reliability remains sensitive to illumination, visibility, scale, and occlusion. Large-scale benchmarks such as Caltech, CityPersons [7], and EuroCity Persons [8] have driven substantial progress with dense pedestrian annotations in urban traffic scenes. However, these datasets are still dominated by daytime or favourable lighting conditions. Although ECP includes night images, daytime samples remain much more common. This creates a clear domain shift problem, detectors trained mainly on daytime data often degrade at night due to reduced visibility, glare, noise, and large illumination differences.

Night-time perception is commonly addressed through low-light enhancement or day-to-night translation. Enhancement methods improve visibility of images already captured at night. For example, LightDiff [9] uses diffusion-based enhancement with perception-aware guidance to favour outputs that improve detector performance. However, such methods enhance existing night-time images rather than generate new labelled night-time samples for augmentation. Day-to-night translation instead converts labelled daytime images into night-style images so that the original annotations can be reused. Early approaches used GAN-based pipelines [10], [11], later augmenting them with semantic, geometric, and depth-based constraints to better preserve scene layout under severe illumination changes. Bang et al. [12], for instance, use semantic segmentation and depth cues in a structure-aware CycleGAN-style framework. More recent diffusion-based methods improve fidelity and practicality: CycleGAN-Turbo [13] enables efficient one-step unpaired translation, while Seed-to-Seed Translation [14] operates in the latent seed space of a pretrained diffusion model to improve structural correspondence in driving scenes.

These works are closely related to our goal, but most focus on perceptual realism, reconstruction quality, or overall task performance, with limited explicit attention to pedestrian-level annotation consistency. In contrast, we treat day-to-night translation as a source-annotation-preserving augmentation strategy for pedestrian detection, rather than as night-style

transfer alone. To this end, we introduce Contrastive-SDXL, a diffusion-based framework that combines target-domain realism with semantic- and object-level preservation through patch-wise correspondence in an external feature space and a novel object-level consistency loss. Beyond visual quality, we evaluate whether the generated images improve downstream night-time pedestrian detection compared with real night-time data and existing day-to-night translation methods, providing empirical evidence for the usefulness of Contrastive-SDXL.

B. Consistency-preserving unpaired translation

Preserving spatial and semantic correspondence between the source input and translated output remains a central challenge in unpaired image-to-image translation. CycleGAN by Jun-Yan Zhu et al. [10] uses forward and backward mappings with adversarial losses and a cycle-consistency loss to enforce approximate reconstruction. While effective, this requires bidirectional generators and discriminators, and does not explicitly preserve small or detector-critical objects under large appearance shifts such as day-to-night scenes [15].

Patch-wise contrastive learning provides an alternative. CUT [16] replaces explicit cycle-consistency with PatchNCE, which maximises mutual information between corresponding local regions in the input and translated images, enabling one-sided unpaired translation with improved content preservation. Later works refine what should be preserved and how negatives should be constructed. F/LSeSim [17] argues that direct feature matching can be brittle under large appearance changes, and instead preserves spatial self-similarity patterns. NEGCUT [18], PUT [19], and MoNCE [20] improve contrastive learning through adversarial hard negatives, ranking and pruning, or negative reweighting. Building on these ideas, Jung et al. [5] proposed to preserve semantic relations among patches using semantic relation consistency regularisation and hard negative mining.

These contrastive formulations are relevant for pedestrian preservation because pedestrians in urban traffic scenes are often small, occluded, and embedded in cluttered backgrounds. However, most existing contrastive translation methods rely on GAN-based encoder–decoder generators, whose intermediate features can be directly used for patch matching. Although diffusion-based generators provide stronger priors, their stochastic noise injection and denoising make intermediate U-Net features less stable for semantic comparison between source and translated images. To combine diffusion priors with relation-preserving objectives such as SRC and hDCE, we use an external encoder for patch-wise semantic matching. Motivated by evidence that self-supervised vision transformers learn object-level patch representations without manual labels [21], we adopt DINOv2 [6] to measure semantic correspondence independently of the generator.

III. PROBLEM FORMULATION AND DESIGN OBJECTIVES

This work aims to develop an annotation-preserving cross-domain augmentation framework for safety-critical perception, focusing on night-time pedestrian detection using latent diffusion models. We consider an unpaired setting where the source

domain, daytime, contains abundant labelled data, while the target domain, night-time, contains only limited samples.

Let the source and target datasets be

$$X_S = \{(x_S^i, y_S^i)\}_{i=1}^N, \quad X_T = \{(x_T^j, y_T^j)\}_{j=1}^M, \quad N \gg M, \quad (1)$$

where $x_S, x_T \in \mathbb{R}^{H \times W \times C}$ denote source and target images, and y_S, y_T their bounding-box annotations.

Our goal is to learn a mapping

$$G_\theta : S \rightarrow T \quad (2)$$

that translates daytime images into visually coherent night-time images while preserving scene semantics. We generate synthetic night-time samples as

$$\hat{x}_T^i = G_\theta(x_S^i), \quad i = 1, \dots, N, \quad (3)$$

forming

$$\hat{X}_T = \{(\hat{x}_T^i, y_S^i)\}_{i=1}^N, \quad (4)$$

where source annotations are reused and the generated samples are expected to follow the target-domain distribution:

$$p(\hat{x}_T) \approx p(x_T). \quad (5)$$

However, safety-critical augmentation requires more than visually realistic target-domain images. A translated image may appear night-time yet be unsuitable for detector training if pedestrians are distorted, erased, or semantically misaligned. We therefore define five design objectives: target-domain alignment, semantic consistency, object-of-interest integrity, efficient adaptation, and synthetic data reliability.

- 1) **Target-domain distribution alignment:** Generated images should match the visual characteristics and statistical distribution of real night-time data.
- 2) **Semantic consistency and invariance:** Translation should preserve source-image semantics, including objects and their spatial relationships.
- 3) **Object-of-interest integrity:** Pedestrians should remain visible, spatially aligned, and structurally consistent after translation.
- 4) **Efficient adaptation:** The model should adapt to the target domain with minimal training cost while retaining the generative capacity of the pretrained diffusion model.
- 5) **Synthetic data reliability:** Low-quality samples containing artefacts or missing critical objects should be filtered before augmentation.

IV. PROPOSED METHOD

To address these objectives, we propose **Contrastive-SDXL**, a diffusion-based cross-domain augmentation framework that translates daytime images into realistic night-time images while preserving semantic structure and pedestrian integrity. The generator is adapted to the night-time domain using Low-Rank Adaptation (LoRA) and trained with four complementary objectives: a DINOv2-guided patch-wise semantic contrastive loss, a detector-guided object consistency loss, an adversarial target-domain alignment loss, and an identity regularisation term. Figure 1 gives an overview of the framework.

A. Generator Backbone and Efficient Adaptation

To satisfy **target-domain alignment**, Contrastive-SDXL builds on SDXL-Turbo [3], a one-step pretrained latent diffusion model with a strong generative prior. Given a source image x_S , the generator encodes it into a latent representation

$$z_S = \text{VAE}_{enc}(x_S). \quad (6)$$

Noise is injected according to the diffusion noise schedule:

$$\tilde{z}_S = \alpha_t z_S + \sigma_t \epsilon, \quad (7)$$

where ϵ is sampled noise, and α_t and σ_t are timestep-dependent scaling coefficients. The noisy latent is processed by the text-conditioned UNet denoiser and decoded back to image space:

$$\hat{x}_T = \text{VAE}_{dec}(f_\theta(\tilde{z}_S, t, c)), \quad (8)$$

where f_θ denotes the UNet-based denoising function and c is the text prompt embedding.

Although this pathway provides strong target-domain realism, its internal features are optimised for denoising rather than explicit semantic correspondence. This motivates the use of an external semantic encoder for contrastive supervision.

To satisfy **efficient adaptation**, we use LoRA [4] instead of fully fine-tuning SDXL-Turbo. Given a pretrained weight matrix $W_0 \in \mathbb{R}^{d \times k}$, LoRA decomposes the update ΔW as

$$\Delta W = AB, \quad r \ll \min(d, k), \quad (9)$$

where $A \in \mathbb{R}^{d \times r}$ and $B \in \mathbb{R}^{r \times k}$ are trainable, giving

$$W = W_0 + \Delta W. \quad (10)$$

Following Parmar et al. [13], we also use encoder–decoder skip connections to preserve fine-grained spatial structure, which is critical when source annotations must remain valid after translation.

B. Patch-Wise Semantic Contrastive Supervision with DINOv2

To ensure **semantic consistency and invariance**, we adopt the Patch-wise Semantic Contrastive Learning framework for Unpaired Translation (PSCUT) proposed by Jung et al. [5]. Unlike CycleGAN [10], which requires forward and reverse mappings, PSCUT operates with a single mapping $G : S \rightarrow T$ and preserves content through patch-level semantic relations. It consists of Semantic Relations Consistency Loss (SRC) and hard Negative Contrastive Loss (hDCE).

a) *Semantic Relations Consistency Loss:* Let z_s^k and z_t^k denote patch features from the source image x_S and translated image \hat{x}_T . SRC preserves the relative semantic relationships between z_s^k and the other patches $\{z_s^i\}$ in the source image with the relationships between their corresponding patches z_t^k and $\{z_t^i\}$ in the translated image. These pairwise relationships define a similarity distribution over patches. For source and translated patches, the similarity distributions are

$$S_k(i) = \frac{\exp(z_s^{k\top} z_s^i)}{\sum_{j=1}^{N_p} \exp(z_s^{k\top} z_s^j)}, \quad T_k(i) = \frac{\exp(z_t^{k\top} z_t^i)}{\sum_{j=1}^{N_p} \exp(z_t^{k\top} z_t^j)}, \quad (11)$$

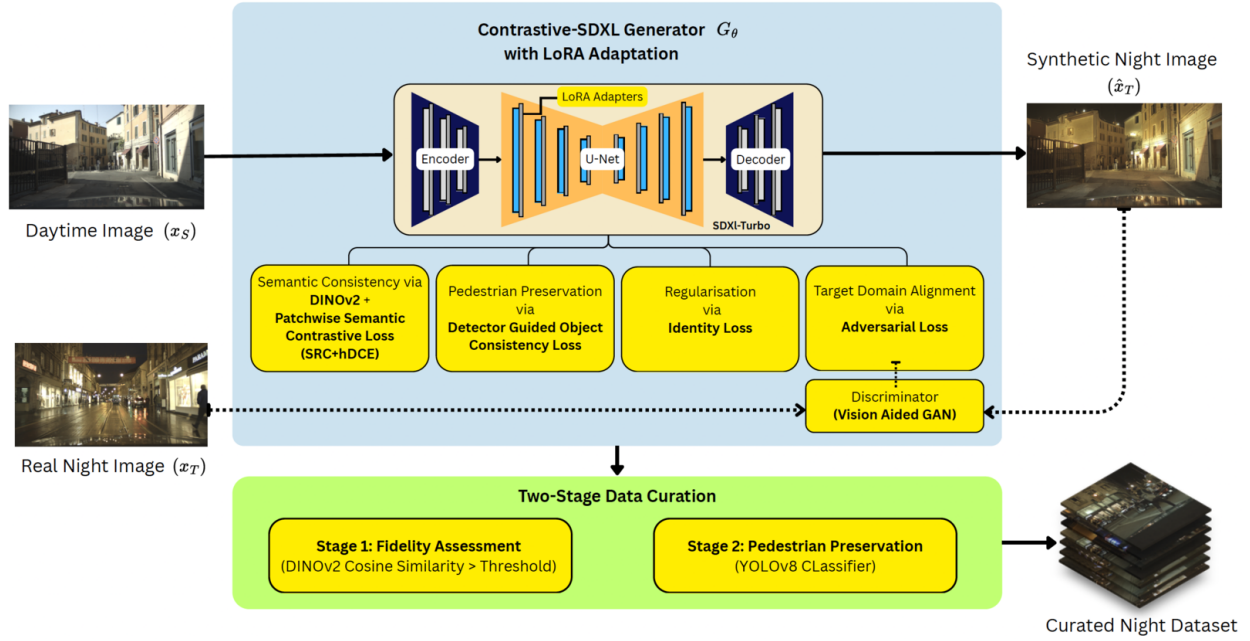


Figure 1: Overview of Contrastive-SDXL. A daytime image x_S is translated into a synthetic night-time image \hat{x}_T using an SDXL-Turbo generator G_θ with LoRA adaptation. The model is guided by patch-wise semantic contrastive loss, detector-guided object consistency, identity regularisation, and adversarial alignment. A two-stage curation pipeline filters generated images using DINOv2 similarity and YOLOv8 pedestrian preservation before detector training.

where N_p is the number of patches. The SRC loss is then computed as the Jensen-Shannon divergence between these similarity distributions:

$$L_{SRC} = \sum_{k=1}^{N_p} \text{JSD}(S_k \parallel T_k). \quad (12)$$

b) Hard Negative Contrastive Loss: Complementing SRC, hDCE pulls corresponding source and translated patches closer while pushing non-matching patches apart. For a query patch z_t^k , the positive sample is the corresponding source patch z_s^k , while $\{z_s^j\}_{j \neq k}$ serve as negatives. hDCE maximises the similarity of the positive pair (z_s^k, z_t^k) while minimising similarity to hard negatives. These hard negatives are semantically similar patches from different spatial locations, providing a stronger contrastive signal.

For a positive pair (z_t^k, z_s^k) and negative patches $\{z_s^j\}_{j \neq k}$, the loss is

$$L_{hDCE}(\gamma, \tau) = \mathbb{E}_{(z_t, z_s) \sim p_{z_s z_t}} [-\log R(z_t, z_s)], \quad (13)$$

$$R(z_t, z_s) = \frac{\exp(z_t^\top z_s / \tau)}{N \mathbb{E}_{z_s^- \sim q_{z_s^-}} [\exp(z_t^\top z_s^- / \tau)]},$$

where τ is the temperature and γ controls the hardness of negative sampling. In practice, hard negatives are sampled from patches in the same image that have high semantic similarity to the query patch. Given the normalised source feature map $\hat{\mathbf{F}}_S \in \mathbb{R}^{N_p \times d}$, the intra-image semantic similarity matrix is computed as

$$\mathbf{M} = \hat{\mathbf{F}}_S \hat{\mathbf{F}}_S^\top, \quad (14)$$

where M_{ij} is the cosine similarity between patches i and j . The semantic weighting matrix is then derived as

$$W_{ij} = \frac{\exp(M_{ij}/\gamma)}{\sum_{k=1}^{N_p} \exp(M_{ik}/\gamma)}, \quad (15)$$

which defines the sampling distribution for hard negatives.

c) DINOv2 External Encoder: A key modification in our framework is the source of patch features. In the original PSCUT framework, patch-wise contrastive losses are applied to generator encoder features, an approach that is suitable for deterministic GAN-based networks but less effective for diffusion models, where stochastic noise injection and denoising make intermediate U-Net features unreliable for semantic comparison. As shown in Figure 4, Contrastive-SDXL variants trained using self-attention maps from different levels of UNet_{enc} fail to maintain semantic correspondence, often producing artefacts, distortions, and poor pedestrian preservation.

We therefore use a frozen pretrained DINOv2 semantic encoder [6], denoted DINO_{enc}, to extract semantic and context-aware patch features. Given a source image $x_S \sim X_S$ and its translated counterpart $\hat{x}_T = G(x_S)$, both images are passed through DINO_{enc}. For each selected layer $l \in L$, we obtain hidden states

$$F_S^l, F_T^l \in \mathbb{R}^{N_l \times C_l}, \quad (16)$$

where N_l is the number of patch tokens after discarding special tokens. We sample N_p patch indices from each feature map and apply a layer-specific two-layer MLP projection head

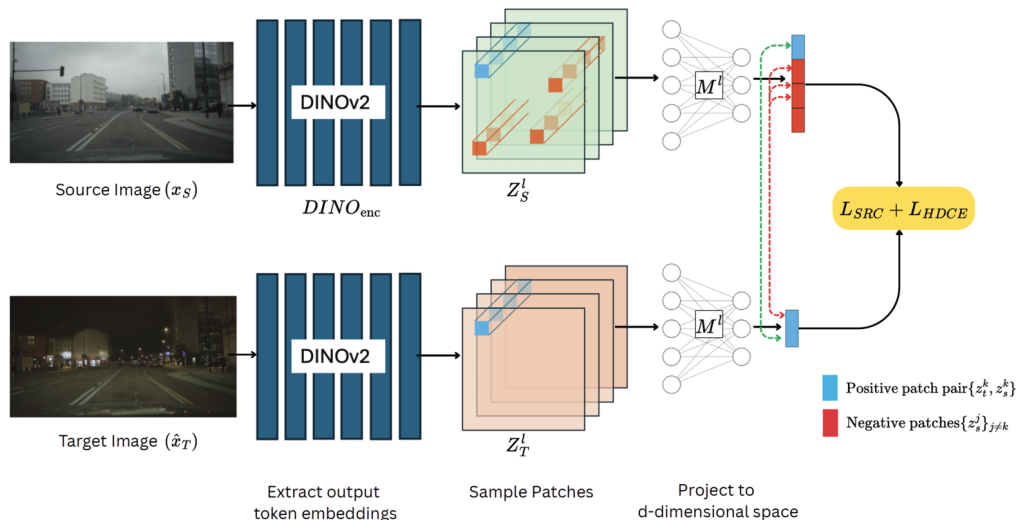


Figure 2: DINOv2 encoder used to extract multi-level semantic features for patch-wise contrastive loss computation.

M^l to map the selected features into a shared d -dimensional embedding space:

$$f_S^l = M^l(F_S^l[p]), \quad f_T^l = M^l(F_T^l[p]), \quad p \in \Omega_l, \quad (17)$$

where $\Omega_l \subseteq \{1, \dots, N_l\}$ is the set of sampled patch indices. Patch-wise contrastive losses are computed across all selected layers, treating corresponding spatial locations as positives and other patches as negatives, as illustrated in Figure 2. Aggregating the losses across multiple DINOv2 layers encourages preservation of both local structure and higher-level semantics, leading to night-time images that are more reliable for downstream pedestrian detector training.

C. Detector-Guided Object Consistency Loss

The contrastive objective encourages semantic consistency at local and global levels, but does not explicitly guarantee that pedestrians remain detectable after translation. This is critical for pedestrian augmentation. To enforce **object-of-interest integrity**, we introduce a detector-guided object consistency loss that encourages the generator to preserve pedestrian-specific visual cues using a pretrained YOLO11 detector finetuned on EuroCity Persons (ECP) [8]. The detector is kept fixed and used only to provide task-specific supervision to the generator.

Given a translated image $\hat{x}_T = G(x_S)$ and source annotations $Y_S = \{y_i\}_{i=1}^N$, where each annotation contains a pedestrian class label and bounding box $y_i = [c_i, b_i]$, we pass \hat{x}_T through the detector and compute the detection loss against Y_S . If \hat{x}_T preserves the source geometry, the original bounding boxes should remain valid. The detector-guided loss is computed using the standard YOLO objective:

$$L_{\text{det}} = \lambda_{\text{box}} L_{\text{box}} + \lambda_{\text{cls}} L_{\text{cls}} + \lambda_{\text{dfl}} L_{\text{dfl}}, \quad (18)$$

where L_{box} , L_{cls} , and L_{dfl} denote the bounding box regression, classification, and distribution focal losses, respectively [22]. We use the default YOLO11 weights $\lambda_{\text{box}} = 7.5$, $\lambda_{\text{cls}} = 0.5$, and $\lambda_{\text{dfl}} = 1.5$.

Here, L_{box} penalises localisation errors between predicted and source bounding boxes using CIoU-style regression [23]. L_{cls} encourages pedestrian regions in the translated image to remain distinguishable from the background, while L_{dfl} refines localisation by modelling bounding box coordinates as discrete distributions. The loss is computed from the detector's raw training outputs before non-maximum suppression to preserve differentiability.

Gradients from L_{det} are propagated through the frozen detector to the generator, encouraging translations in which pedestrians remain visible, well localised, and detectable.

D. Adversarial Target-Domain Alignment

While the pretrained diffusion model captures a broad natural image prior, this alone does not guarantee alignment with the specific appearance of real night-time scenes. Therefore, to further enforce **Target-domain alignment**, we introduce an adversarial domain-alignment objective L_{adv} to ensure that translated images resemble the target night-time domain rather than only preserving source content.

A discriminator D_ϕ is trained to distinguish real night-time images $x_T \sim X_T$ from translated images $\hat{x}_T = G_\theta(x_S)$. Following Vision-Aided GAN [24], we augment the discriminator with features from a frozen CLIP image encoder, providing high-level perceptual cues for separating real and synthetic night-time images.

The discriminator is trained to maximise

$$L_D = \mathbb{E}_{x_T \sim X_T} [\log D_\phi(x_T)] + \mathbb{E}_{x_S \sim X_S} [\log(1 - D_\phi(G_\theta(x_S)))], \quad (19)$$

while the generator minimises

$$L_{\text{adv}} = \mathbb{E}_{x_S \sim X_S} [\log(1 - D_\phi(G_\theta(x_S)))]. \quad (20)$$

Together with the pretrained diffusion prior, this objective encourages target-domain realism, while the contrastive and detector-guided losses preserve pedestrian-relevant structure.

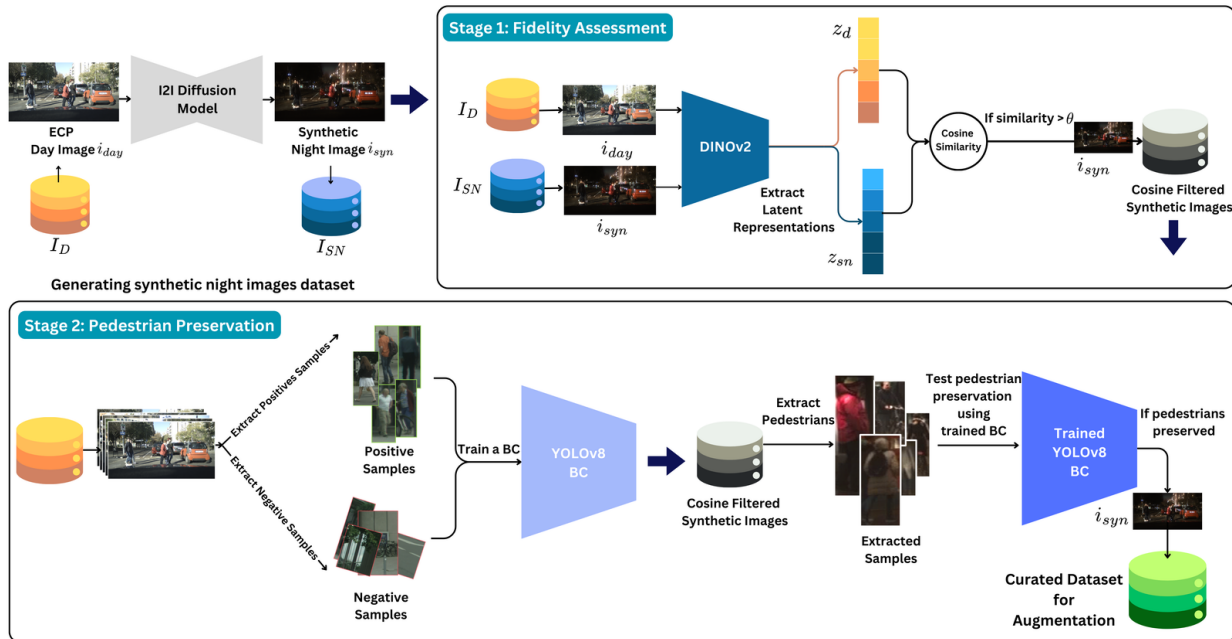


Figure 3: Overview of the two-stage curation pipeline used to filter synthetic night-time images before data augmentation.

E. Identity Regularisation

We also include an identity regularisation term to discourage unnecessary changes when the input already belongs to the target domain. Given a night-time image $x_T \sim X_T$, the generator is encouraged to reconstruct it with minimal alteration:

$$L_{\text{idt}} = \mathbb{E}_{x_T \sim X_T} [\|G_\theta(x_T) - x_T\|_1]. \quad (21)$$

This helps separate domain transfer from content corruption and complements the contrastive, detector-guided, and adversarial objectives.

F. Two-Stage Data Curation

Even with the above supervision, some generated images may contain artefacts, semantic misalignments, or pedestrian distortions. Since metrics such as FID do not measure whether critical objects are preserved, we introduce a two-stage curation pipeline to ensure **synthetic data reliability**.

a) Stage 1: Fidelity Assessment: In the first stage, we assess whether each translated image remains semantically faithful to its source. For each source–translation pair, we extract DINOv2 features and compute their cosine similarity. The acceptance threshold is calibrated on a disjoint held-out set of 250 daytime images and their translated counterparts, manually labelled as accepted or rejected based on overall scene-semantic preservation and whether the source annotations remain usable. We select the threshold that maximises the F1 score against these labels. In our experiments, this threshold was 0.95. Translations below the threshold are discarded.

b) Stage 2: Pedestrian Preservation: The remaining samples are then checked for explicit pedestrian preservation. We train a YOLOv8-based binary classifier [25] to classify cropped patches as pedestrian or background. Positive crops are taken from source pedestrian bounding boxes, while

negative crops are sampled from pedestrian-free regions and verified using a rectangle intersection test to avoid overlap with any pedestrian instance. At inference time, we crop translated images at the inherited source bounding-box locations and evaluate each patch with the classifier. If any expected pedestrian patch is classified as background, the translated image is discarded.

The full curation pipeline is shown in Figure 3. It ensures that the final synthetic set is not only target-like, but also faithful to the source scene and compatible with inherited pedestrian annotations.

G. Full Objective

The overall objective of Contrastive-SDXL combines the patch-wise semantic contrastive losses, detector-guided object consistency, identity regularisation, and adversarial alignment:

$$L_{\text{total}} = \lambda_{\text{SRC}} L_{\text{SRC}} + \lambda_{\text{hDCE}} L_{\text{hDCE}} + \lambda_{\text{det}} L_{\text{det}} + \lambda_{\text{idt}} L_{\text{idt}} + \lambda_{\text{adv}} L_{\text{adv}}. \quad (22)$$

Here, each λ controls the contribution of its corresponding loss term. The contrastive losses L_{SRC} and L_{hDCE} preserve semantic structure and local patch correspondence, L_{det} enforces pedestrian-level consistency, L_{idt} discourages unnecessary changes to images, while the adversarial loss L_{adv} aligns generated images with the real night-time distribution.

By jointly optimising these objectives, Contrastive-SDXL encourages target-domain realism, semantic consistency, and pedestrian preservation, making the generated images more reliable for downstream night-time pedestrian detection.

V. EXPERIMENTS

A. Dataset and Baselines

We use the EuroCity Persons (ECP) dataset [8], a large-scale pedestrian detection benchmark with over 238,200 person

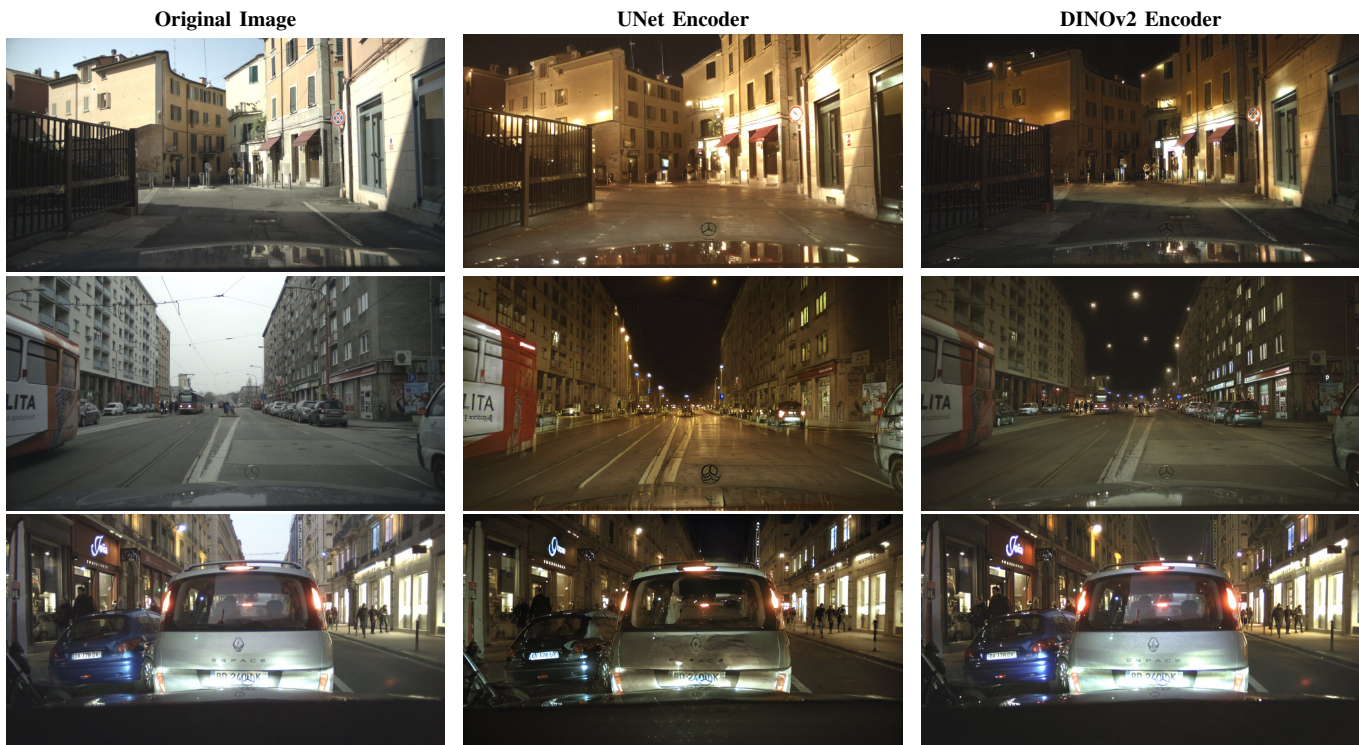


Figure 4: Comparison of night-time images generated using Contrastive-SDXL with UNet encoder features (middle column) versus DINOv2 encoder features (right column). The left column shows the original daytime images. Using DINOv2 features leads to better preservation of pedestrian details and overall image quality.

instances across 47,300 urban images. Since our task is daytime-to-night-time translation, ECP is suitable because it provides both daytime data for source-domain training and real night-time images for adaptation and evaluation. Although datasets such as NightOwls [26] were considered, the lack of publicly available detectors trained on them makes fair comparison difficult. ECP is widely used in pedestrian detection research and provides established baselines and pretrained models, making it appropriate for evaluating whether daytime-trained detectors benefit from synthetic night-time data.

We compare Contrastive-SDXL with two off-the-shelf LDM-based image-to-image translation models, InstructPix2Pix [27] and CycleGAN-Turbo [13]. Both are used to translate ECP daytime images into night-time counterparts and serve as baselines for evaluating whether pretrained LDMs can act as augmentation tools for low-light pedestrian detection.

B. Pedestrian Detectors

We evaluate two downstream detectors, Pedestron [28] and YOLO26 [29], to assess the effectiveness of synthetic night-time images. Pedestron is a pedestrian-specific detector with established ECP performance, while YOLO26 provides a complementary general detector for testing whether the effects of synthetic augmentation generalise across architectures.

For Pedestron, we use the Cascade Mask R-CNN [30] variant with an HRNet backbone, initialised from an ECP-day checkpoint. This checkpoint serves as the baseline and is fine-tuned on the night-time adaptation sets, including real, synthetic, and mixed real-synthetic data, rather than trained from scratch.

For YOLO26, we first train a pretrained YOLO26x model on the ECP daytime training split at resolution 1280, then fine-tune it on real night-time images, synthetic night-time images, or mixed real-synthetic data. All validation is performed on the real ECP night-time validation split. YOLO26 fine-tuning is staged by first freezing most of the backbone, then unfreezing intermediate layers, and finally training the full network with a lower learning rate and mosaic augmentation disabled.

Across both detectors, we evaluate four adaptation settings: the daytime baseline on the ECP day and night validation splits to measure the domain gap; fine-tuning on curated synthetic night-time images only, to test whether generated data alone can support target-domain adaptation; fine-tuning on mixed sets with curated synthetic images and increasing proportions of real night-time data, reflecting settings where only limited target-domain data are available; and fine-tuning on real ECP night-time images as an upper-bound reference. All detectors are evaluated using the ECP-style log-average miss rate (LAMR) protocol, with detections matched to ground truth at an IoU threshold of 0.5 and miss rate averaged over FPPI points from 10^{-2} to 10^0 . Results are reported on the Reasonable, Small, Occluded, and All subsets, following the standard ECP pedestrian detection convention.

C. Contrastive-SDXL Training Details

We follow a training setup similar to PSCUT, with modifications for the diffusion-based generator, DINOv2-based patch-wise contrastive learning, and the detector-guided object consistency loss L_{det} . To adapt SDXL-Turbo, LoRA modules

are inserted into the UNet cross-attention layers, transformer MLP projection layers, convolutional layers, and all layers of the VAE encoder and decoder.

Table I: FID and Wasserstein Distance (WD) between synthetic night-time images from different models and real ECP night-time images. Lower values indicate higher fidelity and closer distributional alignment. Real ECP subsets are included to contextualise WD values. Best synthetic results are shown in bold, and “-” denotes cases where the metric is not applicable.

Model / Dataset	Reference Distribution	Day → Night	
		FID ↓	WD ↓
InstructPix2Pix [27]		64.11	31.8
CycleGAN-Turbo [13]	ECP Night	38.36	37.4
Contrastive-SDXL		22.57	11.27
ECP Day	ECP Night	-	34.8
ECP Night subset 1	ECP Night subset 2	-	5.6

We first tested patch-wise contrastive loss computation using self-attention features from every fourth UNet encoder layer to capture both local and global context. However, these features produced artefacts and weak preservation of fine details, as shown in Figure 4. We therefore use a frozen DINOv2 ViT-G/14 encoder for contrastive supervision. Forward hooks are attached to the last five transformer blocks, excluding the final block. For hidden states of shape $[B, N_l, C_l]$, where $N_l = H_l W_l + 1$ includes the [CLS] token, the special token is removed and the remaining patch embeddings are reshaped into feature maps $F^l \in \mathbb{R}^{B \times C_l \times H_l \times W_l}$.

Before DINOv2 feature extraction, x_S and \hat{x}_T are resized to 504×504 . For each selected layer $l \in L$, we sample 128 spatial indices from the translated feature map and use the same indices for the source feature map, ensuring spatially aligned positives. Each feature level is processed by a layer-specific two-layer MLP projection head M^l :

$$f_S^l(p) = M^l(F_S^l[p]), \quad f_T^l(p) = M^l(F_T^l[p]), \quad (23)$$

producing 256-dimensional L2-normalised features. All other sampled locations in the batch act as negatives. InfoNCE is computed at each layer and summed across selected layers. During training, DINOv2 remains frozen; only the LoRA adapters, skip-connection convolutions, and projection MLPs are updated. As shown in Figure 4, DINOv2 features preserve semantic correspondence and pedestrian details more effectively than UNet encoder features.

For hard negative sampling, SRC computes semantic relation weights between source patches, which modulate the hDCE objective by prioritising semantically meaningful negatives. Both λ_{SRC} and λ_{hDCE} are linearly ramped from 0 to 1 over the first 12,000 iterations, and the hDCE concentration parameter is set to $\gamma = 0.5$.

For object consistency, we use a YOLO11 detector fine-tuned offline on a small annotated subset of ECP daytime and night-time images. The detector is frozen during Contrastive-SDXL training, and L_{det} is computed on dense predictions before confidence thresholding and non-maximum suppression, allowing gradients to propagate through the detector to the generator.

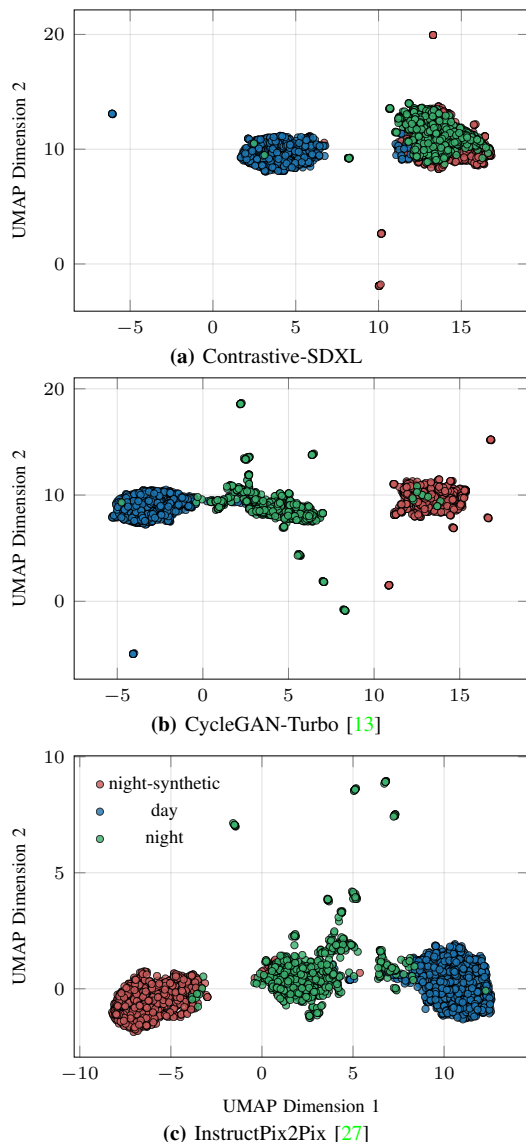


Figure 5: Two-dimensional UMAP visualisation of real daytime, real night-time, and synthetic night-time images for three generative models. Contrastive-SDXL synthetic images cluster closer to real night-time images than the other generated sets, indicating improved distributional alignment.

The generator and discriminator are trained using Adam with learning rate $1e^{-5}$ and weight decay $1e^{-2}$ for 25,000 steps, batch size 1, on an NVIDIA A100 GPU. Loss weights are set to $\lambda_{\text{SRC}} = 1.0$, $\lambda_{\text{hDCE}} = 1.0$, $\lambda_{\text{det}} = 0.5$, $\lambda_{\text{idt}} = 0.1$, and $\lambda_{\text{adv}} = 0.01$.

InstructPix2Pix and CycleGAN-Turbo are used in their default configurations without fine-tuning. Since InstructPix2Pix resizes ECP images from 1920×1024 to 576×320 , bounding boxes are scaled by 0.3 in width and 0.3125 in height. In total, 4,266 ECP daytime validation images are translated by all models and curated using the proposed two-stage pipeline. We construct training sets using synthetic images only, and synthetic images mixed with 5%, 10%, and 20% real night-time data.

The pretrained Pedestron model is fine-tuned on each

Table II: Pedestrian detection performance on the ECP night validation set under different night-time augmentation settings. Results are reported as log-average miss rate across occlusion levels. The baseline model (BM) highlights the day-to-night domain gap, while fine-tuned models use synthetic night-time images from different image-to-image LDMs with varying real night augmentation ratios. The ratio denotes the percentage of real ECP night-time images mixed with synthetic images; 0% indicates purely synthetic augmentation. The Target Model, fine-tuned on the full ECP night-time training set, serves as an upper-bound reference. Best synthetic results are shown in bold.

Pedestrian Detector	I2I-Model	Real night injection ratio (%)	Validation Dataset	Reasonable ↓	Small ↓	Heavy ↓	All ↓	
Pedestron-BM [28]	–	–	ECP Day	4.0	10.0	24.0	14.0	
	–	–	ECP Night	11.0	17.0	31.0	20.0	
Fine-tuned Models	Contrastive-SDXL	0%	ECP Night	9.0	14.0	25.0	16.0	
		5%		8.0	12.0	25.0	15.0	
		10%		8.0	11.0	24.0	15.0	
		20%		8.0	11.0	23.0	14.0	
	CycleGAN-Turbo [13]	0%	ECP Night	14.0	18.0	31.0	21.0	
		5%		11.0	17.0	29.0	18.0	
		10%		10.0	16.0	26.0	17.0	
		20%		9.0	15.0	26.0	16.0	
	InstructPix2Pix [27]	0%	ECP Night	28.0	31.0	46.0	37.0	
		5%		16.0	22.0	41.0	25.0	
		10%		12.0	18.0	33.0	20.0	
		20%		12.0	15.0	31.0	19.0	
Target Model (Pedestron fine-tuned on real night images)	–	100%	ECP Night	7.0	11.0	22.0	14.0	
YOLO-BM [29]	–	–	ECP Day	4.0	11.0	22.0	15.0	
	–	–	ECP Night	10.0	17.0	36.0	19.0	
Fine-tuned Models	Contrastive-SDXL	0%	ECP Night	9.0	16.0	33.0	18.0	
		5%		9.0	14.0	31.0	17.0	
	CycleGAN-Turbo [13]	0%	ECP Night	12.0	20.0	35.0	21.0	
		5%		11.0	18.0	33.0	21.0	
	InstructPix2Pix [27]	0%	ECP Night	18.0	30.0	45.0	29.0	
		5%		15.0	22.0	40.0	25.0	
	Target Model (YOLO fine-tuned on real night images)	–	100%	ECP Night	7.0	13.0	28.0	16.0

augmented set and, for reference, on the full ECP night-time training set. Fine-tuning is performed for 28 epochs with gradual layer unfreezing every fourth epoch, using SGD with learning rate 0.001, momentum 0.9, and weight decay 0.0001.

D. Evaluation Protocols

Synthetic image quality is evaluated using Fréchet Inception Distance (FID) [31] and Wasserstein Distance (WD), both computed between real night-time images and synthetic outputs. Lower values indicate closer target-domain alignment. We also visualise distributional alignment using UMAP [32], embedding ECP daytime, real night-time, and synthetic night-time images from pixel space after resizing them to 240×128 .

Downstream detection performance follows the Pedestron protocol. We report LAMR over FPPI [10^{-2} , 10^0] across the Reasonable, Small, Heavy, and All subsets.

E. Comparison to Baselines and Other LDMs

We compare Contrastive-SDXL with InstructPix2Pix and CycleGAN-Turbo in terms of synthetic image quality and downstream detection performance. FID and WD are reported in Table I, UMAP comparisons are shown in Figure 5, and detector results under different real night injection ratios are

reported in Table II. The daytime-only detector serves as the baseline, while the model trained on full real night-time data serves as the target-domain reference.

1) *Qualitative and Quantitative Image Quality:* Table I shows that Contrastive-SDXL achieves the lowest FID of 22.57, outperforming InstructPix2Pix (64.11) and CycleGAN-Turbo (38.36). It also obtains the lowest WD of 11.27. For reference, the WD between two disjoint subsets of real ECP night-time images is 5.6, indicating that Contrastive-SDXL approaches the distributional characteristics of real night-time data. The UMAP visualisation in Figure 5 shows the same trend, with Contrastive-SDXL samples clustering closer to real night-time images and separating more clearly from daytime samples.

2) *Downstream Detection Performance:* Table II reports detection performance under different augmentation settings. Both daytime-only baselines show a clear drop on night-time images, confirming the day-to-night domain gap. For Pedestron, the All miss rate increases from 14.0% on ECP Day to 20.0% on ECP Night; for YOLO, it increases from 15.0% to 19.0%.

The real night injection ratio denotes the amount of real ECP night-time data added to the synthetic set. For example, 5% injection adds real night-time images equal to 5% of the synthetic set size. This allows us to test whether limited real night-time data can approach full target-domain supervision.

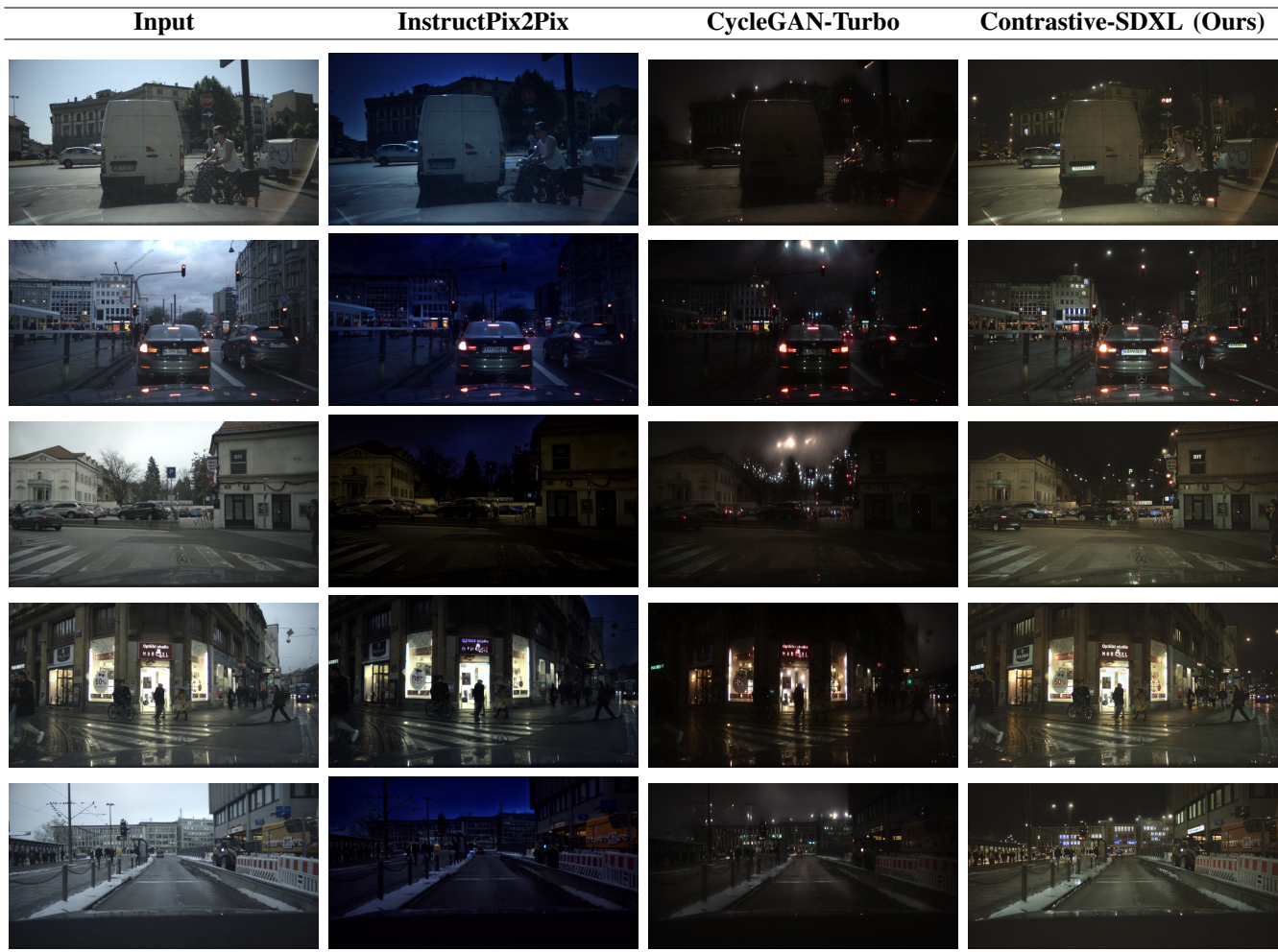


Figure 6: Qualitative comparison of synthetic night-time images generated by InstructPix2Pix, CycleGAN-Turbo, and Contrastive-SDXL. The leftmost column shows the original daytime inputs. CycleGAN-Turbo produces darker night-like images but often loses pedestrian details, while InstructPix2Pix captures night-time lighting but introduces artefacts and inconsistent pedestrian preservation. In contrast, Contrastive-SDXL generates realistic night-time images while preserving critical pedestrian details.

Contrastive-SDXL consistently performs best among the synthetic augmentation methods. Without real night-time data, it reduces the Pedestron All miss rate to 16.0%, outperforming CycleGAN-Turbo (21.0%), InstructPix2Pix (37.0%), and the daytime baseline on ECP Night (20.0%). With 20% real night injection, Contrastive-SDXL reaches 14.0%, matching the model trained on the full real night-time set.

The same trend holds for YOLO. Without real night-time injection, YOLO fine-tuned with Contrastive-SDXL achieves an All miss rate of 18.0%, improving over the YOLO baseline (19.0%) and outperforming CycleGAN-Turbo (21.0%) and InstructPix2Pix (29.0%). With only 5% real night-time injection, Contrastive-SDXL reduces the All miss rate to 17.0%, close to the full real night YOLO target model at 16.0%.

Overall, the results show that Contrastive-SDXL produces synthetic night-time images that are both closer to real night-time data and more useful for downstream detection, with gains observed across both Pedestron and YOLO.

F. Generalisation to Out-of-Distribution Images

To evaluate out-of-distribution generalisation, we test Contrastive-SDXL on daytime images from TJU-DHD [33], which contains urban scenes that differ from ECP. The selected images include varied environments, lighting conditions, and pedestrian appearances. As shown in Figure 7, Contrastive-SDXL captures night-time lighting and atmospheric conditions in these unfamiliar scenes while preserving pedestrian structure and visibility, suggesting generalisation beyond the training domain.

VI. DISCUSSION

The results show that Contrastive-SDXL generates annotation-preserving night-time images that are useful for downstream pedestrian detection. Compared with other pre-trained latent diffusion models, it better preserves scene structure and pedestrian regions while translating the appearance to the night-time domain. This is supported by the qualitative results and by the FID, WD, and UMAP analyses, which show closer alignment with real night-time data.



Figure 7: Example daytime images from TJU-DHD (left) and their night-time translations generated by Contrastive-SDXL (right). Contrastive-SDXL effectively captures night-time lighting while preserving pedestrian details, even in out-of-distribution urban scenes.

More importantly, these improvements translate into stronger detection performance. Both Pedestron and YOLO benefit from fine-tuning with Contrastive-SDXL images, suggesting that the augmentation is not tied to a single detector architecture. This is important for safety-critical pedestrian perception, where synthetic data should improve detector robustness rather than visual realism alone. The translated TJU-DHD examples further suggest generalisation to out-of-distribution urban scenes.

Overall, these findings support Contrastive-SDXL as a practical augmentation framework for low-light pedestrian detection. The results also indicate that pretrained LDMs require explicit consistency-preserving constraints before they can be reliably used for safety-critical detection. Future work should examine whether similar gains transfer to other transportation tasks, including traffic sign recognition and road-object detection under adverse illumination, weather and occlusions. Since YOLO shows more modest gains than Pedestron, future work should also study how detector architecture, fine-tuning strategy, and the mixture of real and synthetic target-domain data affect adaptation performance.

VII. CONCLUSION

This work presents Contrastive-SDXL, a diffusion-based day-to-night augmentation framework for safety-critical pedestrian detection. By combining DINOv2-guided semantic contrastive learning with detector-guided object consistency, the method generates night-time images that preserve pedestrian annotations while aligning with the target night-time domain.

Experiments with Pedestron and YOLO show that these images improve downstream night-time pedestrian detection, demonstrating their usefulness beyond visual realism alone.

REFERENCES

- [1] C. Saharia, W. Chan, H. Chang, C. Lee, J. Ho, T. Salimans, D. Fleet, and M. Norouzi, “Palette: Image-to-image diffusion models,” in *ACM SIGGRAPH 2022 conference proceedings*, 2022, pp. 1–10.
- [2] C. Meng, Y. He, Y. Song, J. Song, J. Wu, J.-Y. Zhu, and S. Ermon, “Sdedit: Guided image synthesis and editing with stochastic differential equations,” *arXiv preprint arXiv:2108.01073*, 2021.
- [3] A. Sauer, D. Lorenz, A. Blattmann, and R. Rombach, “Adversarial diffusion distillation,” in *European Conference on Computer Vision*. Springer, 2024, pp. 87–103.
- [4] E. J. Hu, Y. Shen, P. Wallis, Z. Allen-Zhu, Y. Li, S. Wang, L. Wang, and W. Chen, “Lora: Low-rank adaptation of large language models,” *arXiv preprint arXiv:2106.09685*, 2021.
- [5] C. Jung, G. Kwon, and J. C. Ye, “Exploring patch-wise semantic relation for contrastive learning in image-to-image translation tasks,” in *Proceedings of the IEEE/CVF conference on computer vision and pattern recognition*, 2022, pp. 18 260–18 269.
- [6] M. Oquab, T. Darcet, T. Moutakanni, H. Vo, M. Szafraniec, V. Khalidov, P. Fernandez, D. Haziza, F. Massa, A. El-Nouby *et al.*, “Dinov2: Learning robust visual features without supervision,” *arXiv preprint arXiv:2304.07193*, 2023.
- [7] S. Zhang, R. Benenson, and B. Schiele, “Citypersons: A diverse dataset for pedestrian detection,” in *Proceedings of the IEEE conference on computer vision and pattern recognition*, 2017, pp. 3213–3221.
- [8] M. Braun, S. Krebs, F. Flohr, and D. M. Gavrilu, “The eurocity persons dataset: A novel benchmark for object detection,” *arXiv preprint arXiv:1805.07193*, 2018.
- [9] J. Li, B. Li, Z. Tu, X. Liu, Q. Guo, F. Juefei-Xu, R. Xu, and H. Yu, “Light the night: A multi-condition diffusion framework for unpaired low-light enhancement in autonomous driving,” in *Proceedings of the IEEE/CVF Conference on Computer Vision and Pattern Recognition*, 2024, pp. 15 205–15 215.
- [10] J.-Y. Zhu, T. Park, P. Isola, and A. A. Efros, “Unpaired image-to-image translation using cycle-consistent adversarial networks,” in *Proceedings of the IEEE international conference on computer vision*, 2017, pp. 2223–2232.
- [11] A. Anoosheh, T. Sattler, R. Timofte, M. Pollefeys, and L. Van Gool, “Night-to-day image translation for retrieval-based localization,” in *2019 International conference on robotics and automation (ICRA)*. IEEE, 2019, pp. 5958–5964.
- [12] G. Bang, J. Lee, Y. Endo, T. Nishimori, K. Nakao, and S. Kamijo, “Semantic and geometric-aware day-to-night image translation network,” *Sensors*, vol. 24, no. 4, 2024. [Online]. Available: <https://www.mdpi.com/1424-8220/24/4/1339>
- [13] G. Parmar, T. Park, S. Narasimhan, and J.-Y. Zhu, “One-step image translation with text-to-image models,” *arXiv preprint arXiv:2403.12036*, 2024.
- [14] O. Greenberg, E. Kishon, and D. Lischinski, “Seed-to-seed: Image translation in diffusion seed space,” *arXiv preprint arXiv:2409.00654*, 2024.
- [15] C.-T. Lin, S.-W. Huang, Y.-Y. Wu, and S.-H. Lai, “Gan-based day-to-night image style transfer for nighttime vehicle detection,” *IEEE Transactions on Intelligent Transportation Systems*, vol. 22, no. 2, pp. 951–963, 2021.
- [16] T. Park, A. A. Efros, R. Zhang, and J.-Y. Zhu, “Contrastive learning for unpaired image-to-image translation,” in *European conference on computer vision*. Springer, 2020, pp. 319–345.
- [17] C. Zheng, T.-J. Cham, and J. Cai, “The spatially-correlative loss for various image translation tasks,” in *Proceedings of the IEEE/CVF conference on computer vision and pattern recognition*, 2021, pp. 16 407–16 417.
- [18] W. Wang, W. Zhou, J. Bao, D. Chen, and H. Li, “Instance-wise hard negative example generation for contrastive learning in unpaired image-to-image translation,” in *Proceedings of the IEEE/CVF international conference on computer vision*, 2021, pp. 14 020–14 029.
- [19] Y. Lin, S. Zhang, T. Chen, Y. Lu, G. Li, and Y. Shi, “Exploring negatives in contrastive learning for unpaired image-to-image translation,” in *Proceedings of the 30th ACM international conference on multimedia*, 2022, pp. 1186–1194.
- [20] F. Zhan, J. Zhang, Y. Yu, R. Wu, and S. Lu, “Modulated contrast for versatile image synthesis,” in *Proceedings of the IEEE/CVF Conference on Computer Vision and Pattern Recognition*, 2022, pp. 18 280–18 290.

- [21] M. Caron, H. Touvron, I. Misra, H. Jégou, J. Mairal, P. Bojanowski, and A. Joulin, "Emerging properties in self-supervised vision transformers," in *Proceedings of the IEEE/CVF international conference on computer vision*, 2021, pp. 9650–9660.
- [22] X. Li, W. Wang, L. Wu, S. Chen, X. Hu, J. Li, J. Tang, and J. Yang, "Generalized focal loss: Learning qualified and distributed bounding boxes for dense object detection," *Advances in neural information processing systems*, vol. 33, pp. 21 002–21 012, 2020.
- [23] Z. Zheng, P. Wang, W. Liu, J. Li, R. Ye, and D. Ren, "Distance-iou loss: Faster and better learning for bounding box regression," in *Proceedings of the AAAI conference on artificial intelligence*, vol. 34, no. 07, 2020, pp. 12 993–13 000.
- [24] N. Kumari, R. Zhang, E. Shechtman, and J.-Y. Zhu, "Ensembling off-the-shelf models for gan training," in *Proceedings of the IEEE/CVF conference on computer vision and pattern recognition*, 2022, pp. 10 651–10 662.
- [25] G. Jocher, A. Chaurasia, and J. Qiu, "Ultralytics YOLO," Jan. 2023. [Online]. Available: <https://github.com/ultralytics/ultralytics>
- [26] L. Neumann, M. Karg, S. Zhang, C. Scharfenberger, E. Piegert, S. Mistr, O. Prokofyeva, R. Thiel, A. Vedaldi, A. Zisserman, and B. Schiele, "Nightowls: A pedestrians at night dataset," in *Computer Vision – ACCV 2018, Lecture Notes in Computer Science*, vol. 11361. Springer, Cham, 2019, pp. 691–705.
- [27] T. Brooks, A. Holynski, and A. A. Efros, "Instructpix2pix: Learning to follow image editing instructions," in *Proceedings of the IEEE/CVF Conference on Computer Vision and Pattern Recognition*, 2023, pp. 18 392–18 402.
- [28] I. Hasan, S. Liao, J. Li, S. U. Akram, and L. Shao, "Generalizable pedestrian detection: The elephant in the room," in *Proceedings of the IEEE/CVF Conference on Computer Vision and Pattern Recognition*, 2021, pp. 11 328–11 337.
- [29] G. Jocher and J. Qiu, "Ultralytics yolo26," 2026. [Online]. Available: <https://github.com/ultralytics/ultralytics>
- [30] Z. Cai and N. Vasconcelos, "Cascade r-cnn: High quality object detection and instance segmentation," *IEEE transactions on pattern analysis and machine intelligence*, vol. 43, no. 5, pp. 1483–1498, 2019.
- [31] M. Heusel, H. Ramsauer, T. Unterthiner, B. Nessler, and S. Hochreiter, "Gans trained by a two time-scale update rule converge to a local nash equilibrium," in *Advances in neural information processing systems*, vol. 30, 2017.
- [32] L. McInnes, J. Healy, and J. Melville, "Umap: Uniform manifold approximation and projection for dimension reduction," *arXiv preprint arXiv:1802.03426*, 2018.
- [33] Y. Pang, J. Cao, Y. Li, J. Xie, H. Sun, and J. Gong, "Tju-dhd: A diverse high-resolution dataset for object detection," *IEEE Transactions on Image Processing*, vol. 30, pp. 207–219, 2020.

Franky George Franky George is currently pursuing the Ph.D. degree at the University of Hull, U.K. His research focuses on generative models, particularly diffusion-based models, with an emphasis on disentangling latent spaces to improve controllability in generative modelling. He received the master's degree in artificial intelligence and data science from the University of Hull. He has secured research grants supporting collaborative work with the University of Bologna, where he investigated the capabilities and limitations of diffusion models in mimicking and understanding famous artistic styles. His research contributes to both the theoretical understanding and practical application of generative models.

Muhammad Khalid Muhammad Khalid is an Assistant Professor at the University of Hull, U.K. His research focuses on robotic autonomy and safety, with particular emphasis on human-robot interaction in agricultural environments. Before joining the University of Hull, he was a Post-Doctoral Research Fellow at the University of Lincoln, where he worked on the MeSAPro project to improve robotic safety in strawberry harvesting. He received the Ph.D. degree from Northumbria University in 2020, where his research focused on autonomous parking systems for smart cities under a fully funded studentship. His work contributes to robotics, agricultural automation, and smart city infrastructure.

Adil Khan Adil Khan is a Professor of Machine Learning and Artificial Intelligence with more than 16 years of experience in AI research, development, and teaching. His expertise spans traditional machine learning and deep learning, with applications in natural language processing, medical image analysis, crime detection, and related industrial and theoretical challenges. His research includes the development of efficient document-ranking mechanisms and robust data-augmentation methods for deep neural networks. He has secured substantial research funding from organizations including Huawei and the Analytical Center of Artificial Intelligence at Innopolis University. His work focuses on improving the generalization, adaptability, and security of machine learning models.